STOCHASTIC ANALYSIS OF URBAN V2X COMMUNICATIONS: ORTHOGONALITY VERSUS NON-ORTHOGONALITY

Zhenhui Situ[1], Ivan Wang-Hei Ho[1], Xiaoli Xu[2], Yong Liang Guan[3], and Cao Ding[1]
[1]Department of Electronic and Information Engineering, The Hong Kong Polytechnic University, Hong Kong, China, [2]School of Information Science and Engineering, Southeast University, Nanjing 210096, China, [3]School of Electrical and Electronic Engineering, Nanyang Technological University, Singapore 639801

NOTE: Corresponding author: I. W.-H. Ho, ivanwh.ho@polyu.edu.hk

Abstract – *In this paper, we study the broadcasting performance of urban Vehicle-to-everything (V2X) communications at road intersections. In such environments, dense buildings obstruct the radio channel between vehicles in adjacent road segments and Non-Line-Of-Sight (NLOS) signal propagation reduces the received power level. Therefore, messages that originate from adjacent roads traveling in a non-parallel directions usually have weaker signals than those from the road segment traveling in parallel opposite direction. Besides, the high vehicular density leads to insufficient orthogonal channel resources and high level of interference. We propose to apply Non-Orthogonal Multiple Access (NOMA) to V2X communications at urban road intersections to enhance the spectrum efficiency and improve the Package Delivery Ratio (PDR) performance. With NOMA, signals from multiple transmitters are decoded together and the interference from undesired users can be canceled if these messages are retrieved. Specifically, we study two NOMA-based V2X communication schemes, namely, NOMA-V2X decoded by Successive Interference Cancellation (SIC-V2X) and NOMA-V2X decoded by Joint Decoding (JD-V2X). Based on the tools developed in stochastic geometry, we derive and compare the PDR expressions for both NOMA schemes and the Orthogonal Multiple Access (OMA) scheme. Our results indicate that 1) both NOMA schemes outperform the conventional OMA scheme and the PDR of LOS/NLOS communications with two-user access increases by 51%/369%; 2) for four-user access, the proposed NOMA scheme shows 375% goodput enhancement as compared with the OMA scheme; and 3) JD-V2X provides significant PDR enhancement compared with SIC-V2X in the high data rate regime. Finally, we also demonstrate that the random access based NOMA schemes can achieve lower transmission latency than collision-free scheduling schemes when the road is over 56% jammed.*

Keywords – Joint decoding (JD), non-orthogonal multiple access (NOMA), stochastic analysis, successive interference cancellation (SIC), vehicle-to-everything (V2X)

1. INTRODUCTION

[1] Today vehicles are smarter than ever to cooperate with each other to offer a safe and high-quality driving experience, and together they form a Cooperative Intelligent Transportation System (C-ITS) to provide various services. Vehicle-to-everything (V2X) communications, as the cornerstone of C-ITS, is expected to provide low-latency and reliable communications in a high-dense dynamic environment for high-level applications. Dedicated Short-Range Communications (DSRC) and Cellular Vehicle-to-everything (C-V2X) are two distinct regimes in V2X communications. DSRC is regarded as the beginning of V2X and supports direct communications via the IEEE 802.11p standard. The C-V2X was released by the Third Generation Partnership Project (3GPP) group to enable support from the widely deployed Long Term Evolution (LTE) or 5G networks for V2X [1]. DSRC only supports decentralized resource allocations while C-V2X can allocate resources in both centralized and distributed manners, referred to as modes 3 and 4 respectively.

However, as the number of on-road wireless users keeps growing, it leads to serious aggregated interference. This may significantly degrade the communication quality and lead to high transmission latency. The problem deteriorates further when the Line-Of-Sight (LOS) path between the transmitter and receiver is obstructed by buildings or other obstacles, which is common in dense urban areas. To mitigate the problem by harnessing interference, Non-Orthogonal Multiple Access (NOMA) is recently considered for V2X communications [2]. Compared with conventional Orthogonal Multiple Access (OMA) where radio resources are assigned in an orthogonal manner, NOMA allows multiple users to exploit the spectrum resources concurrently, thus achieving high spectral efficiency and low transmission latency [3]. In addition, cooperative NOMA is verified to have better outage performance for multi-pair information exchange compared with existing OMA schemes [4]. It can also interplay with other emerging technologies, such as massive Multiple-Input Multiple-Output (MIMO), cooperative communications, and energy harvesting, to enhance driving safety [5].

[1]This work was supported in part by the General Research Fund (Project No. 15201118) established under the University Grant Committee (UGC) of the Hong Kong Special Administrative Region (HKSAR), China; and by The Hong Kong Polytechnic University (Project No. 1-ZVTJ).

Successive Interference Cancellation (SIC) is a Multiuser Decoder (MUD) technology that was widely considered in NOMA systems. It decodes multiple users in sequence according to their received signal strengths. The strongest user who has the highest received power level is decoded first while other users are regarded as interference. After a user is successfully decoded, the corresponding signal is subtracted from the superimposed signal for decoding the subsequent users. In addition to SIC, another well-known MUD is Joint Decoding (JD). In JD, the overlapping signals of all transmitters are jointly decoded. Fig. 1 shows the power regions of the two-user uplink Additive White Gaussian Noise (AWGN) channel, within which SIC and JD can decode successfully [6].

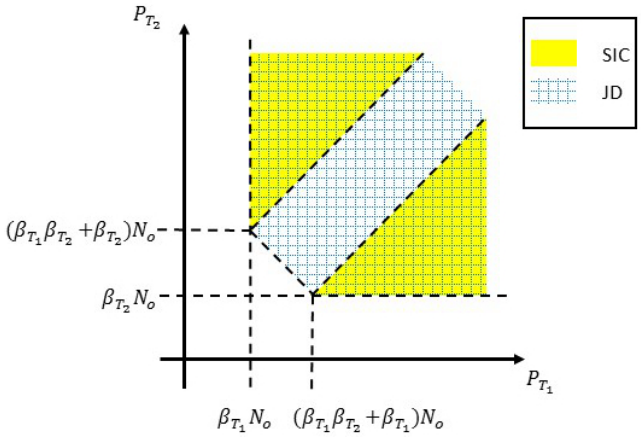

Fig. 1 – Power region of the two-user uplink AWGN channel that are decodable by SIC and JD, respectively. The notations are elaborated in Table 1.

The power region that the two users can be successfully decoded with SIC is divided into two parts. The upper-left region indicates that user 2 is the strong user while the lower-right region indicates that user 1 is the strong user. We can observe from Fig. 1 that the power region of JD is larger than that of SIC. By allowing the power levels of the two users to be balanced, JD provides a larger power region and higher probability to decode the two users. Since SIC decodes one user at one time, the complexity of SIC approximately scales linearly with the number of users. On the other hand, the complexity of JD grows exponentially with the number of users [7]. Therefore, JD provides better performance than SIC at the cost of higher complexity. Network-Coded Multiple Access (NCMA) is an example of JD-based NOMA scheme that employs Physical-layer Network Coding (PNC) to boost the throughput [8][9]. Focusing on message exchange among multiple vehicles, our previous work showed that NCMA provided higher throughput performance as compared with SIC and the complexity can be reduced by exploiting the side information [10][11].

For SIC, certain power difference is required among the interfering users to ensure that the interference from the weak users does not fail the signal decoding of the strong user. There is a rich body of papers on resource allocation and power control algorithms for SIC-based NOMA to guarantee the power difference [12, 13, 14]. Several recent pieces of work on NOMA in V2X communications also considered SIC-based NOMA [2, 13, 15]. They studied the power difference problem and proposed several centralized resource allocation algorithms to address the issue.

However, centralized resource allocation and power control are not always available in V2X communications. For example, it is infeasible in areas without the coverage of base stations. Besides, centralized control requires additional signaling overheads, which may be fatal for time-critical applications. For the delivery of relatively small-sized packages, centralized control may seriously degrade the transmission efficiency. In such cases, decentralized resource allocation is a better choice. However, the performance of NOMA operation in an uncoordinated network is unclear. To fill the gap, this paper aims to apply NOMA to V2X operating in an uncoordinated network and evaluate the performance. Stochastic geometry is exploited to capture critical performance metrics of the vehicular networks, such as the distribution of interfering vehicles, the shadow fading, and Package Delivery Ratio (PDR), by taking the potential geometrical patterns of on-road units into consideration. To this end, this paper provides a tractable network model for applying NOMA to V2X in an urban area, and proposes optimization methods to maximize the overall network goodput. Our main contributions are summarized as follows:

1. We develop a comprehensive network model with three Multiuser Access (MUA) schemes, including OMA, SIC-based NOMA, and JD-based NOMA, for V2X communications at a road intersection. This model characterizes the practical vehicular channel by considering the impact of obstacles. It enables tractable analysis for applying NOMA to V2X efficiently without requiring the time-consuming Monte Carlo method.
2. The analytical results obtained from the network model are validated by extensive simulations, with practical settings. The results illustrate that the two NOMA schemes outperform the OMA scheme when the target user suffers with a poor radio channel, which might be caused by NLOS and long-distance transmission. The PDR, which is lower than 0.2 with the use of OMA, increases up to 0.55 and 0.75 with the use of SIC and JD, respectively. For the strong user with a good radio channel, JD provides up to 20% and 30% PDR enhancement compared with SIC and OMA, respectively. Overall, both analytical and simulation results reveal that NOMA can significantly improve the communication quality when the target radio channel is poor.
3. Based on our analytical results, we propose a data rate optimization scheme to maximize the overall goodput by balancing the data rate and PDR. The formulated optimization algorithm can be implemented very efficiently, which is feasible for time-critical V2X applications.

4. The proposed random access schemes are compared with the benchmark with Collision-Free Scheduled Access (CFSA). The simulation results reveal that the NOMA schemes can achieve lower transmission latency than CFSA when the road is over 56% jammed.

The rest of this paper is organized as follows. Section 2 reviews related work on NOMA and V2X communications. The network model, channel model, and receiver design are described in Section 3. In Section 4, the analytical expressions of PDR are derived and analyzed using stochastic geometry. A data rate optimization algorithm to maximize the goodput is also proposed in Section 4. Section 5 provides numerical results to validate the network model and evaluate the proposed algorithm. Finally, we conclude this paper in Section 6.

2. RELATED WORK

This paper focuses on applying NOMA to V2X communications, in which the network is uncoordinated and vehicles independently select radio resources based on random channel access. The performance of NOMA with random access was studied in several recent pieces of work [16, 17, 18, 19]. Choi [16] applied NOMA to multichannel ALOHA with multiple subchannels and multiple power levels, and proved that the proposed scheme achieved higher goodput than the conventional OMA-based multichannel ALOHA. Seo et al. [17] studied NOMA random access with multiple levels of target power based on channel inversion. Compared with conventional random access without power control, the proposed scheme improved the maximum goodput from 0.368 to 0.7. NOMA random channel access with Rayleigh fading channel was investigated in [18], where a backlogged UE randomly aims at one of the received powers at the base station with channel inversion. The authors applied SIC with multilevel target powers, and both the lower bound on the throughput and the upper bound on the mean access delay were improved. [19] considered not only SIC but also JD for random access. The simulation revealed that the two techniques showed similar performance over frequency-flat Block-Fading Multiple Access Channel (BF-MAC), but JD provided higher outage-limited maximum goodput than SIC. Since NOMA was mainly studied for cellular networks, [16, 17, 18, 19] focused on unicast communication with a single receiver. However, one of the main applications of V2X communications is safety message broadcasting, in which the performance of multiple users within a certain region should be considered.

When applying NOMA to V2X communications, the characteristics of vehicles need to be captured and studied to ensure the feasibility of NOMA in vehicular networks. Di et al. [20, 2] applied NOMA to alleviate the performance degradation in terms of latency and packet reception probability caused by the high density of vehicles. Focusing on SIC-based NOMA, they proposed a scheme including both centralized subchannel allocation and distributed transmission power adjustment for V2X broadcasting to minimize the latency and maximize the packet reception probability. The proposed algorithm, was suboptimal since the formulated problem was NP-hard, and only simulation results were provided to evaluate the performance. The authors in [15] studied the dynamic cell association caused by the high vehicle mobility and dynamic communication environment. They deployed SIC-based NOMA and proposed an algorithm to jointly optimize the cell association and power control to maximize the long-term system utility. In [21], the authors considered the strong user as a relay for the weak user via exploiting the side information for interference cancellation. A similar concept was extended in [22] by considering MIMO Spatial Modulation (MIMO-SM) and Vehicle-to-Vehicle (V2V) networks. In [13], the authors considered heterogeneous vehicular communications consisting of V2V, Vehicle-to-Infrastructure (V2I), and femto-user to femto-station (F2FS) links. SIC-based NOMA was exploited in vehicular networks and an optimized power allocation scheme was proposed to improve the goodput and reliability. However, most of this prior work relied on centralized control and did not consider any mathematically tractable network model; the proposed algorithms can only be evaluated via time-consuming simulation. Besides, they primarily focused on SIC receivers without much discussion on JD-based NOMA.

In light of the inadequacy, it is important to obtain a tractable network model to study the feasibility and performance of NOMA in V2X communications. To this end, we conduct a comprehensive study that considers NOMA in V2X communications with not only the SIC decoder, which is widely assumed in NOMA systems, but also the JD decoder.

3. SYSTEM MODELS

The notations in this paper are summarized in Table 1.

3.1 Network model

To accurately capture the characteristic of V2X communications in urban areas, this paper analyzes the performance of the proposed scheme using stochastic geometry [23]. This tool had been widely used to model V2X communications [24, 25]. We consider a V2X communication scenario at a road intersection as illustrated in Fig. 2.

All vehicles on the road intersection want to broadcast messages, which are either Basic Safety Messages (BSMs) to share the local information such as position, heading, and speed [26] or multimedia content for infotainment services. We study the PDR of messages from transmitters within the communication Range of Interest (ROI) with radius r. Without loss of generality, the receiver is considered to be located on road segment E. The maximum distance between the receiver and the center point

Table 1 – Notations

Notations	Definition
x_o	Distance between the receiver and the center point of the road intersection
x_{T_i}	Distance between the receiver and transmitter T_i
r	Communication range of interest
K	Number of users to decode for MUD
Ω_j	Set of target transmitters on street EW or NS ($j = 1$ or 2)
Ω	Set of target transmitters, $\Omega = \Omega_1 \cup \Omega_2$
$\Omega_{T_i}^{SIC}$	Set of possible transmitter combinations to decode user T_i with SIC
$\Omega_{T_i}^{JD}$	Set of possible transmitter combinations to decode user T_i with JD
λ	Density of interfering vehicles on each street (one sub-channel)
Φ_j	Set of interfering vehicles on street EW or NS ($j = 1$ or 2)
Υ	The set of distances between transmitters and receiver
α_j	Path loss exponent for vehicles on street EW or NS ($j = 1$ or 2)
ρ_j	Path loss for vehicles on street EW or NS ($j = 1$ or 2)
h_{T_i}	Rayleigh fading for vehicle T_i on either street EW or NS
P_{tx}	Transmitter power
P_{T_i}	Received power of transmitter T_i
$\mathcal{I}_j$	Aggregated interference from vehicles on street EW or NS ($j = 1$ or 2) apart from target transmitters
$\mathcal{R}_{T_i}^{max}$	Maximum achievable data rate of transmitter T_i
β_{T_i}	Minimum SINR to decode signal from transmitter T_i
N_o	Power level of thermal noise

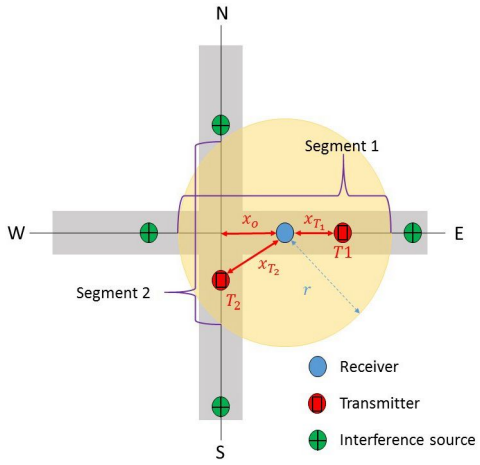

Fig. 2 – V2X communications at a road intersection.

of the road intersection is assumed as x_o^{max}. We focus on the case that the ROI involves two users from the two streets NS and EW, which means $r \geq x_o^{max}$, and evaluate the PDR of messages on the two segments. This paper derives the PDR for MUD given an arbitrary number of target transmitters, based on which we can study the performance of MUD under different access scenarios. Let Ω_1 and Ω_2 denote the sets of target transmitters on streets EW and NS, respectively.

When the vehicular density is high [2], the MAC protocol can be approximated as ALOHA according to [24]. This paper focuses on V2X communications in dense networks, thus ALOHA is assumed in the following analysis. Since the transmission range of the vehicles is much larger than the width of the road, vehicles on the two streets EW and NS can be modeled by two one dimensional (1-D) homogeneous Poisson Point Processes (PPPs) with density (intensity) λ on each subchannel. Besides the set of target transmitters $\Omega = \Omega_1 \cup \Omega_2$, the sets of interference sources on the two streets are denoted by Φ_1 and Φ_2, respectively. Let the Euclidean distances from the receiver to the center of the intersection and transmitter T_i be x_o and x_{T_i} respectively. We assume that all nodes are uniformly distributed on the road segments, and the Cumulative Distributive Functions (CDFs) of x_o and x_{T_i} are as follows:

$$F_{x_o}(x_o) = \frac{x_o}{x_o^{max}}, \tag{1}$$

$$F_{x_{T_i}|x_o}(x_{T_i}|x_o) = \begin{cases} \frac{x_{T_i}}{r}, & T_i \in \Omega_1 \\ \frac{\sqrt{x_{T_i}^2 - x_o^2}}{\sqrt{r^2 - x_o^2}}, & T_i \in \Omega_2 \end{cases} \tag{2}$$

Hence, the corresponding Probability Density Functions (PDFs) can be written as

$$f_{x_o}(x_o) = \frac{1}{x_o^{max}}, \tag{3}$$

$$f_{x_{T_i}|x_o}(x_{T_i}|x_o) = \begin{cases} \frac{1}{r}, & T_i \in \Omega_1 \\ \frac{x_{T_i}}{\sqrt{(x_{T_i}^2 - x_o^2)(r^2 - x_o^2)}}, & T_i \in \Omega_2 \end{cases} \tag{4}$$

The PDF of transmitters on street NS (e.g., $T_i \in \Omega_2$) depends on the location of the receiver. Let T_{EW} and T_{NS} be

[2] The high density scenario is the most concerning since the PDR usually meets the requirement when the density is low.

two transmitters on streets EW and NS respectively (e.g., $T_{EW} \in \Omega_1$ and $T_{NS} \in \Omega_2$). When the receiver is located at the center point of the intersection, the PDFs of $x_{T_{EW}}$ and $x_{T_{NS}}$ become equivalent. Since the variables $x_{T_{EW}}$ and $x_{T_{NS}}$ are independent, the probability that $x_{T_{EW}} > x_{T_{NS}}$ can be written as

$$\begin{aligned} &Pr(x_{T_{EW}} > x_{T_{NS}} | x_o) \\ =&\int_{x_o}^{r} \int_{x_o}^{T_{EW}} f_{x_{T_{EW}}|x_o}(x_{T_{EW}}|x_o) \\ &\times f_{x_{T_{NS}}|x_o}(x_{T_{NS}}|x_o) dx_{T_{NS}} dx_{T_{EW}} \\ =&\frac{1}{2} + \underbrace{\frac{x_o^2}{2r\sqrt{r^2-x_o^2}} \ln\left(\frac{x_o}{r+\sqrt{r^2-x_o^2}}\right)}_{\text{Monotonically decreasing and negative}}. \end{aligned} \quad (5)$$

Given $x_o \in (0, x_o^{max})$, the second component of the result is negative and monotonically decreasing. For cases that $x_o = 0$ and $x_o = x_o^{max}$, the probabilities of the event $x_{T_{EW}} > x_{T_{NS}}$ are 0.5 and 0, respectively. Generally, it is more likely that $x_{T_{EW}}$ is smaller than $x_{T_{NS}}$, especially when the distance between the center of the intersection and the receiver is large. It means that vehicles on the perpendicular street suffer longer transmission distance.

3.2 Channel and interference models

The transmitted signals from the target vehicles undergo path loss and fast fading, the received power is denoted as P_{T_i}

$$P_{T_i} = h_{T_i} \overline{P}_{T_i} = \begin{cases} h_{T_i} P_{tx} \rho_1 x_{T_i}^{-\alpha_1}, & T_i \in \Omega_1 \\ h_{T_i} P_{tx} \rho_2 x_{T_i}^{-\alpha_2}, & T_i \in \Omega_2 \end{cases} \quad (6)$$

where P_{tx} is the transmitter power, $\alpha_j, j \in \{1,2\}$ is the path loss exponent related to the propagation environment, and ρ_j denotes the path loss at the reference distance one meter away. h_{T_i} is caused by Rayleigh fading with unit mean $\mathbb{E}(h_{T_i}) = 1$, and it follows the exponential distribution $Pr(h_{T_i}) = e^{-h_{T_i}}$. $\overline{P}_{T_i}$ denotes the average received power level. When obstruction exists between the two streets, the received signal on the other street suffers higher α_j, and the previous subsection shows that the transmission distance for $T_i \in \Omega_1$ is usually smaller than that of $T_j \in \Omega_2$. Therefore, P_{T_i} for $T_i \in \Omega_1$ is very likely larger than P_{T_j}, for $T_j \in \Omega_2$. In this paper, conventional receivers decoding the message from T_j and regards the signal from T_i as noise are defined as OMA receivers. When the orthogonality cannot be guaranteed in V2X communications, OMA receivers suffer from low SINR and PDR [27].

In addition to the signals from the NOMA group Ω, the signals from other transmitters lead to interference. Let us focus on one subchannel, the aggregated interferences from vehicles on the two streets are

$$\mathcal{I}_j = \begin{cases} \sum_{T_i \in \Phi_1} h_{T_i} P_{tx} \rho_1 x_{T_i}^{-\alpha_1}, & j = 1 \\ \sum_{T_i \in \Phi_2} h_{T_i} P_{tx} \rho_2 x_{T_i}^{-\alpha_2}, & j = 2 \end{cases} \quad (7)$$

The signals from interference sources have the same path loss exponents and reference power as the desired signals given in *(6)*.

3.3 Receiver design

The current LTE-V applies OMA for V2X communications, most research work on broadcasting either assume interference-free or regards the interference from other transmitters as noise. However, the interference-free assumption is not reasonable when the density of vehicles is high. When we decode $T_j \in \Omega_2$ in Fig. 2, the interference from $T_i \in \Omega_1$ has a large impact on the PDR, which will be elaborated on later. To exploit the collided signals on the same subchannel, NOMA is a potential technique to decode not only the strong user with a higher power level but also the weak user with a lower power level. Two types of NOMA receivers are considered in this work, which are based on SIC and JD respectively. To study a general case, we consider decoding a set of users Ω containing K transmitters (i.e., $|\Omega| = K$). The set of distances between the receiver and the transmitters in Ω is denoted by Υ. Let us denote $\Omega_{T_i}^{SIC}$ and $\Omega_{T_i}^{JD}$ as the sets of possible combinations of transmitters including user T_i that are successfully decoded by SIC and JD receivers, respectively. Specifically, the elements in $\Omega_{T_i}^{SIC}$ are vectors ω with a specific order such as $\omega = (T_a, T_b, ..., T_i)$. The vector ω includes all transmitters decoded before T_i and T_i itself. Let $\omega^{-1}(T_j)$ be the index of transmitter T_j in ω. The elements in ω belong to Ω and the last element is always T_i. $\Omega_{T_i}^{JD}$ is similar to $\Omega_{T_i}^{SIC}$, but the difference is that elements in $\Omega_{T_i}^{JD}$ are subsets without a specific order, since decoding order is not important in JD.

3.3.1 OMA receiver

For the conventional OMA receiver, it decodes the message from one vehicle and regards the aggregated signals from other transmitters as noise. The maximum achievable rate from the transmitter T_i is

$$\mathcal{R}_{T_i}^{max} = \log_2\left(1 + \frac{P_{T_i}}{\sum_{T_j \in \Omega \backslash T_i} P_{T_j} + N_o + \mathcal{I}_1 + \mathcal{I}_2}\right), \quad (8)$$

where N_o is the noise power, and $\Omega \backslash T_i$ denotes the set of target transmitters apart from T_i. Given the minimum Signal-to-Interference-plus-Noise Ratio (SINR), β_{T_i}, for successfully decoding user T_i, messages from transmitter T_i can be decoded when the following constraint is satisfied.

Lemma 1 (constraint of OMA receiver): Transmitter T_i can be successfully decoded by the OMA receiver when event $\mathcal{E}_{T_i}^{OMA}$ occurs, which is defined as

$$\mathcal{E}_{T_i}^{OMA}: \frac{P_{T_i}}{\sum_{T_j \in \Omega \backslash T_i} P_{T_j} + N_o + \mathcal{I}_1 + \mathcal{I}_2} \geq \beta_{T_i}. \quad (9)$$

In this paper, the minimum SINR is assumed to be not less than 0 dB, i.e., $\beta_{T_i} \geq 1$. This is because practical V2X

communications normally require a high data rate, which means a high SINR requirement to guarantee that data is sent within a short contact duration. In addition, the assumption helps simplify the derivation. In this case, at most one transmitter in the set Ω can satisfy constraint *(9)* when there are multiple transmitters, i.e., $|\Omega| > 1$. According to the discussion above, the PDR from $T_j \in \Omega_2$ is likely lower than that of $T_i \in \Omega_1$. Therefore, the PDR from $T_j \in \Omega_2$ is lower than 0.5 even in the absence of interference and noise.

3.3.2 SIC receiver

SIC is widely studied and applied in NOMA due to its low complexity. It decodes the user with the highest received power first, which is known as the strongest user, and other users are regarded as interference sources. When the strong user is successfully decoded, the corresponding signal is removed via subtraction, then the weak users can be decoded in the absence of the strong user.

Lemma 2 (constraint of SIC receiver): Transmitter T_i can be successfully decoded by SIC receiver when $\exists\, \omega \in \Omega_{T_i}^{SIC}$ with a specific order such that event $\mathcal{E}_{\omega}^{SIC}$ is satisfied.

$$\mathcal{E}_{\omega}^{SIC}: \begin{cases} \frac{P_{\omega(1)}}{\sum_{T_j \in \Omega \setminus \omega(1)} P_{T_j} + N_o + \mathcal{I}_1 + \mathcal{I}_2} \geq \beta_{\omega(1)}, \\ \frac{P_{\omega(2)}}{\sum_{T_j \in \Omega \setminus \omega(1:2)} P_{T_j} + N_o + \mathcal{I}_1 + \mathcal{I}_2} \geq \beta_{\omega(2)}, \\ \cdots \\ \frac{P_{T_i}}{\sum_{T_j \in \Omega \setminus \omega} P_{T_j} + N_o + \mathcal{I}_1 + \mathcal{I}_2} \geq \beta_{T_i}. \end{cases} \quad (10)$$

Generally, a SIC receiver decides the decoding order based on the power levels. For the strongest user, the SIC receiver decodes it in the same manner as the OMA receiver. According to *(10)*, the strongest user is decoded first and user T_i is decoded as the last one ($\omega(|\omega|) = T_i$). Compared with the OMA receiver, the SIC receiver improves the PDR of the weak user and provides exactly the same performance for the strongest user as the OMA receiver.

3.3.3 JD receiver

Besides SIC, another well-known NOMA receiver is a joint-decoding receiver, which decodes multiple users simultaneously. For the JD receiver, the constraint to decode T_i is as follows.

Lemma 3 (constraint of JD receiver): Transmitter T_i can be successfully decoded by the JD receiver when $\exists\, \omega \in \Omega_{T_i}^{JD}$ so that event $\mathcal{E}_{\omega}^{JD}$ occurs.

$$\mathcal{E}_{\omega}^{JD}: \begin{cases} \frac{P_{\omega(1)}}{\sum_{T_j \in \Omega \setminus \omega} P_{T_j} + N_o + \mathcal{I}_1 + \mathcal{I}_2} \geq \beta_{\omega(1)}, \\ \cdots \\ \frac{P_{T_i}}{\sum_{T_j \in \Omega \setminus \omega} P_{T_j} + N_o + \mathcal{I}_1 + \mathcal{I}_2} \geq \beta_{T_i}, \\ \frac{\sum_{T_m \in \omega} P_{T_m}}{\sum_{T_j \in \Omega \setminus \omega} P_{T_j} + N_o + \mathcal{I}_1 + \mathcal{I}_2} \geq \beta_{\omega}. \end{cases} \quad (11)$$

The last constraint corresponds to the decoding of the joint signal, where $\beta_{\omega} = \prod_{T_j \in \omega}(1 + \beta_{T_j}) - 1$ denotes the minimum SINR of the sum rate. Other constraints in *(11)* correspond to the SINR requirements for each individual user in the presence of interference from other transmitters in Ω that do not belong to ω. The SIC receiver requires the same SINR for the sum rate by adding up all the constraints in *(10)*. However, the independent power requirements of the JD receiver are looser than that of the SIC receiver. Therefore, the JD receiver allows the power levels of multiple transmitters to be balanced and provides a higher PDR than the SIC receiver.

One of the major research topics in NOMA is to guarantee the power difference between the strong and weak users, but it requires additional signaling and overheads, which leads to a higher delay in V2X communications. Grant-free transmission is assumed in this work and the comparison between the two NOMA receivers is conducted. The performance of the three kinds of receivers mentioned above, i.e., OMA, SIC and JD receivers, will be analyzed rigorously in the following sections.

4. PDR ANALYSIS

Based on the system models introduced in the previous section, three schemes for V2X communications at a road intersection are studied in this paper: 1) OMA-V2X; 2) SIC-V2X; and 3) JD-V2X. The PDR of these three schemes is investigated in this section.

4.1 OMA-V2X

According to the OMA receiver described in the previous section, the PDR of transmitter T_i given the location information Υ when OMA-V2X is applied can be written as follows.

Corollary 1 (PDR of OMA receiver): The probability of successful decoding of the signal from transmitter T_i with the OMA receiver is

$$\begin{aligned} &\mathcal{P}_{\text{OMA,T}_\text{i}}(\Upsilon, x_o) = \mathbb{E}[Pr(\mathcal{E}_{T_i}^{OMA})] \\ &= \mathbb{E}[Pr(\frac{P_{T_i}}{\sum_{T_j \in \Omega \setminus T_i} P_{T_j} + N_o + \mathcal{I}_1 + \mathcal{I}_2} \geq \beta_{T_i})] \\ &\overset{(a)}{=} \mathbb{E}[\exp(-\frac{(\sum_{T_j \in \Omega \setminus T_i} P_{T_j} + N_o + \mathcal{I}_1 + \mathcal{I}_2)\beta_{T_i}}{\overline{P}_{T_i}})] \\ &= \exp(-N_o \frac{\beta_{T_i}}{\overline{P}_{T_i}}) \mathcal{L}_{\mathcal{I}_1}(\frac{\beta_{T_i}}{\overline{P}_{T_i}}) \mathcal{L}_{\mathcal{I}_2}(\frac{\beta_{T_i}}{\overline{P}_{T_i}}) \prod_{T_j \in \Omega \setminus T_i} \mathcal{L}_g(\frac{\overline{P}_{T_j}\beta_{T_i}}{\overline{P}_{T_i}}) \\ &= \mathcal{C}(\frac{\beta_{T_i}}{\overline{P}_{T_i}}) \prod_{T_j \in \Omega \setminus T_i} \mathcal{L}_g(\frac{\overline{P}_{T_j}\beta_{T_i}}{\overline{P}_{T_i}}), \end{aligned} \quad (12)$$

where (a) follows the fact that $h_{T_i} \sim \exp(1)$. $\mathcal{L}_g(s) \triangleq \mathbb{E}(e^{-sg})$, $\mathcal{L}_{\mathcal{I}_1}(s) \triangleq \mathbb{E}(e^{-s\mathcal{I}_1})$, and $\mathcal{L}_{\mathcal{I}_2}(s) \triangleq \mathbb{E}(e^{-s\mathcal{I}_2})$ are Laplace transforms of the random fading component and random sum interference from the two streets. For simplification, $\mathcal{C}(s) \triangleq \exp(-N_o s)\mathcal{L}_{\mathcal{I}_1}(s)\mathcal{L}_{\mathcal{I}_2}(s)$ is used to represent the product of the three components. For

the fading component, the Laplace transform can be computed as

$$\mathcal{L}_g(s) = \mathbb{E}(e^{-sg}) = \int_0^\infty e^{-sg} \times e^{-g} dg = \frac{1}{1+s}. \quad (13)$$

For the interference from street EW, the Laplace transform is

$$\begin{aligned}
&\mathcal{L}_{\mathcal{I}_1}(s) = \mathbb{E}[\exp(-s \sum_{T_j \in \Phi_1} h_{T_j} P_{tx} \rho_1 x_{T_j}^{-\alpha_1}] \\
=&\mathbb{E}[\prod_{T_j \in \Phi_1} \exp(-s h_{T_j} P_{tx} \rho_1 x_{T_j}^{-\alpha_1})] \\
\overset{(b)}{=}& \exp(\lambda \int_0^\infty (\mathbb{E}[\exp(-s h_{T_j} P_{tx} \rho_1 x_{T_j}^{-\alpha_1})] - 1) d(2x_{T_j})) \\
\overset{(c)}{=}& \exp(\int_0^\infty \frac{-2\lambda}{1 + (sP_{tx}\rho_1)^{-1} x_{T_j}^{\alpha_1}} dx_{T_j}) \\
\overset{(d)}{=}& \exp(-\frac{2\pi\lambda (sP_{tx}\rho_1)^{\frac{1}{\alpha_1}}}{\alpha_1 sin(\frac{\pi}{\alpha_1})}),
\end{aligned} \quad (14)$$

where (b) is obtained from the Probability Generating Function (PGF) of PPP, (c) follows the Laplace transform of random variable with exponential distribution in *(13)* and (d) is directly from [28].

The Laplace transform of the sum interference from street NS depends on the location of the receiver. Given the distance x_o between the receiver and the center point, the Laplace transform can be computed as

$$\begin{aligned}
&\mathcal{L}_{\mathcal{I}_2}(s) = \mathbb{E}[\exp(-s \sum_{T_j \in \Phi_2} h_{T_j} P_{tx} \rho_2 x_{T_j}^{-\alpha_2}] \\
=& \exp(\lambda \int_0^\infty (\mathbb{E}[\exp(-s h_{T_j} P_{tx} \rho_2 (x_{T_j}^2 + x_o^2)^{-\frac{\alpha_2}{2}})] \\
&- 1) d(2x_{T_j})) \\
=& \exp(\int_0^\infty \frac{-2\lambda}{1 + (sP_{tx}\rho_2)^{-1} (x_{T_j}^2 + x_o^2)^{\frac{\alpha_2}{2}}} dx_{T_j}),
\end{aligned} \quad (15)$$

which is monotonically increasing with x_o. This is intuitively correct that the aggregated interference decreases as the distance between the receiver and the street NS increases, thus improving the PDR. A lower bound *(15)* can be obtained when x_o becomes zero:

$$\mathcal{L}_{\mathcal{I}_2}(s) \leq \mathcal{L}_{\mathcal{I}_2}^{LB}(s) = \exp(-\frac{2\pi\lambda (sP_{tx}\rho_2)^{\frac{1}{\alpha_2}}}{\alpha_2 sin(\frac{\pi}{\alpha_2})}). \quad (16)$$

For the special case when the number of transmitters to be decoded is 2, i.e., $K = 2$ with $T_1 \in \Omega_1, T_2 \in \Omega_2$, we have the PDR of T_1 as follows.

$$\mathcal{P}_{\text{OMA,T}_1}(\Upsilon, x_o) = \frac{\overline{P}_{T_1}}{\overline{P}_{T_1} + \beta_{T_1} \overline{P}_{T_2}} \mathcal{C}(\frac{\beta_{T_1}}{\overline{P}_{T_1}}). \quad (17)$$

4.2 SIC-V2X

When the SIC decoder is applied, the strongest user is decoded in the same way as that of the OMA decoder, thus the same PDR is obtained. For the weak users, SIC eliminates the signal from the strongest user, and thus increases the PDR. For the SIC decoder, we have the following corollary.

Corollary 2 (PDR of SIC receiver): The probability of successful decoding of the signal from transmitter T_i with the SIC receiver is illustrated by *(18)* and *(19)*.

$$\begin{aligned}
\mathcal{P}_{\text{SIC,T}_i}(\Upsilon, x_o) = \sum_{\omega \in \Omega_{T_i}^{SIC}} [\prod_{T_j \in \omega} (\overline{P}_{T_j} q_{T_j})^{-1}] \times [\prod_{T_j \in \Omega \setminus \omega} (1 \\
+ \overline{P}_{T_j} \sum_{T_m \in \omega} \beta_{T_m} q_{T_m})^{-1}] \mathcal{C}(\sum_{T_j \in \omega} \beta_{T_j} q_{T_j}),
\end{aligned} \quad (18)$$

with

$$q_{T_j} = \overline{P}_{T_j}^{-1} + \sum_{T_m = \omega(1)}^{\omega(\omega^{-1}(T_j)-1)} \beta_{T_m} q_{T_m}. \quad (19)$$

Proof. Please refer to Appendix A. □

Considering the special case that $K = 2$ with $T_1 \in \Omega_1, T_2 \in \Omega_2$, we have the PDR of T_1 as follows.

$$\begin{aligned}
\mathcal{P}_{\text{SIC,T}_1}(\Upsilon, x_o) =& \frac{\overline{P}_{T_1}}{\overline{P}_{T_1} + \beta_{T_1} \overline{P}_{T_2}} \mathcal{C}(\frac{\beta_{T_1}}{\overline{P}_{T_1}}) \\
&+ \frac{\overline{P}_{T_2}}{\beta_{T_2} \overline{P}_{T_1} + \overline{P}_{T_2}} \mathcal{C}(\frac{\beta_{T_1}}{\overline{P}_{T_1}} + \frac{\beta_{T_2}(1+\beta_{T_1})}{\overline{P}_{T_2}}).
\end{aligned} \quad (20)$$

The first component on the Right-Hand-Side (RHS) denotes decoding T_1 as the strong user, which is the same as *(17)*. The second component denotes decoding T_1 as the weak user, in which T_2 is first decoded as the strong user and then is canceled. After that, T_1 is decoded without the interference from T_2.

4.3 JD-V2X

Based on *(11)*, we have the following corollary for the JD receiver.

Corollary 3 (PDR of JD receiver): The probability of successful decoding of the signal from transmitter T_i with the JD receiver is shown in *(21)* and *(22)*.

$$\begin{aligned}
&\mathcal{P}_{\text{JD,T}_i}(\Upsilon, x_o) \\
=& \sum_{s=1}^{|\Omega_{T_i}^{JD}|} \sum_{\substack{\omega_{1:s} \in \Omega_{T_i}^{JD} \\ \omega_m \neq \omega_n \\ |\omega_m| \leq |\omega_n| \\ m<n}} (-1)^{s-1} \sum_{\substack{T_{j_1} \in \omega_{I_1} \\ \omega_{I_1} = \omega_1}} \cdots \sum_{\substack{T_{j_s} \in \omega_{I_s} \\ \omega_{I_s} = \omega_s \setminus \omega_{s-1}}} c(\omega_{1:s})
\end{aligned} \quad (21)$$

with

$$c(\omega_{1:s}) = \begin{cases} 0, & \exists\, \omega_m \nsubseteq \omega_n, m < n \\ \frac{a_{T_{j_1}:T_{j_s}} \mathcal{C}(b_{T_{j_1}:T_{j_s}})}{\prod_{T_m \in \Omega \setminus \omega_{1:s}} (1+\overline{P}_{T_m} b_{T_{j_1}:T_{j_s}})}, & Otherwise \end{cases}$$

$$a_{T_{j_1}:T_{j_s}} = \prod_{m=1}^{s} \{ (\prod_{T_n \in \omega_{I_m}} \frac{\overline{P}_{T_n}^{-1}}{\overline{P}_{T_n}^{-1} + b_{T_{j_1}:T_{j_{m-1}}}}) \times (\prod_{T_l \in \omega_{I_m} \setminus T_{j_m}} \frac{\overline{P}_{T_l}^{-1} + b_{T_{j_1}:T_{j_{m-1}}}}{\overline{P}_{T_l}^{-1} - \overline{P}_{T_{j_m}}^{-1}}) \},$$

$$b_{T_{j_1}:T_{j_s}} = \sum_{m=1}^{s} [\beta_{\omega_{I_m}} (\overline{P}_{T_{j_m}}^{-1} + b_{T_{j_1}:T_{j_{m-1}}}) + \sum_{T_n \in \omega_{I_m}} \beta_{T_n} (\overline{P}_{T_n}^{-1} - \overline{P}_{T j_m}^{-1})]. \quad (22)$$

Proof. Please refer to Appendix B. □

For the special case that $K = 2$ with $T_1 \in \Omega_1, T_2 \in \Omega_2$, we have the PDR of T_1 as illustrated in *(23)*.

$$\begin{aligned} &\mathcal{P}_{\text{JD,T}_1}(\Upsilon, x_o) \\ =&\frac{\overline{P}_{T_1}}{\overline{P}_{T_1} + \beta_{T_1}\overline{P}_{T_2}} \mathcal{C}(\frac{\beta_{T_1}}{\overline{P}_{T_1}}) + \frac{\overline{P}_{T_1}}{\overline{P}_{T_1} - \overline{P}_{T_2}} \mathcal{C}(\frac{\beta_{T_1}(1+\beta_{T_2})}{\overline{P}_{T_1}} \\ &+ \frac{\beta_{T_2}}{\overline{P}_{T_2}}) + \frac{\overline{P}_{T_2}}{\overline{P}_{T_2} - \overline{P}_{T_1}} \mathcal{C}(\frac{\beta_{T_1}}{\overline{P}_{T_1}} + \frac{\beta_{T_2}(1+\beta_{T_1})}{\overline{P}_{T_2}}) \\ &- \frac{\overline{P}_{T_1}}{\overline{P}_{T_1} + \beta_{T_1}\overline{P}_{T_2}} \mathcal{C}(\frac{\beta_{T_1}(1+\beta_{T_2})}{\overline{P}_{T_1}} + \frac{\beta_{T_2}}{\overline{P}_{T_2}}). \end{aligned} \quad (23)$$

4.4 Average PDR at the intersection region

According to the individual analysis of the three receivers, the average PDR is obtained as follows.

Corollary 4 (Average PDR): For each kind of receiver, the average probability of successful decoding of the signal from transmitter T_i at the road intersection can be obtained from the individual PDR as

$$\mathcal{P}_{\text{receiver,T}_i} = \int_0^{x_o^{max}} \int_{x_{T_K}^{min}}^{x_{T_K}^{max}} \cdots \int_{x_{T_1}^{min}}^{x_{T_1}^{max}} \mathcal{P}_{\text{receiver,T}_i}(\Upsilon, x_o) f_{x_{T_1}}(x_{T_1}) \ldots f_{x_{T_K}}(x_{T_K}) f_{x_o}(x_o) dx_{T_1} \ldots dx_{T_K} dx_o, \quad (24)$$

where the integral interval depends on the network topology. For the road intersection considered in this paper, the integral interval of a transmitter depends on which street it belongs to and the distance between the receiver and the center point. For instance, the integral intervals of $x_{T_i}, T_i \in \Omega_1$ and $x_{T_j}, T_j \in \Omega_2$ are $[0, r]$ and $[x_o, r]$, respectively. In the next section regarding simulation studies, we consider different scenarios and analyze the performance of the three schemes.

4.5 Optimization of the data rate

In practice, a wireless communication system detects the power level of noise plus interference in the background and prefers an appropriate data rate so that the goodput can be maximized. For conventional OMA schemes, the optimization aims to maximize the goodput for a single broadcaster. However, NOMA-based systems decode multiple users simultaneously, and thus the optimization needs to jointly satisfy the minimum SINR for multiple transmitters. To optimize the PDR and common data rate so that the overall goodput is maximized for multiple users, we propose a data rate selection algorithm for the three V2X schemes. The optimization problem is characterized as follows:

$$\begin{aligned} \mathcal{R}^{opt} &= \arg\max_{\mathcal{R}} (\sum_{T_i \in \Omega} \mathcal{P}_{\text{T}_i}) \mathcal{R} \\ s.t., &\mathcal{R} \in [\mathcal{R}_{min}, \mathcal{R}_{max}] \end{aligned} \quad (25)$$

where $\mathcal{P}_{\text{T}_i}$ can be $\mathcal{P}_{\text{OMA,T}_i}$, $\mathcal{P}_{\text{SIC,T}_i}$, or $\mathcal{P}_{\text{JD,T}_i}$ depending on the decoder design.

The PDR expressions for the three V2X schemes are expressed in *(12)*, *(18)*, and *(21)*, respectively. The average PDR is difficult to obtain as it involves multiple integrals. However, the optimization problem in *(25)* only involves one design variable with a fixed interval, hence we can solve the problem via the single-variable optimization algorithm [29]. In this paper, golden section search and parabolic interpolation are applied to identify the optimal data rate.

5. NUMERICAL RESULTS

This section discusses the numerical results for the three V2X schemes, and the analytical results are validated through simulation based on MATLAB. In particular, the PDR performance at an intersection under diverse configurations is investigated, and the performance of the proposed data rate optimization is evaluated and its impact is studied. We consider the ROI with radius $r = 200$ m, vehicles with maximum distance $x_o^{max} = 100$ m away from the center point of the road intersection are studied. All transmitters broadcast with the same transmission power at 10 dBW with a bandwidth of 10 MHz. The reference path loss is 54.85 dB for LOS propagation and 54.55 dB for NLOS propagation. The path loss exponent is 1.67 for the LOS case and 1.90 for the NLOS case as suggested in [30]. The noise power spectral density is assumed to be -93 dBm/Hz. We define the reference SNR [31] as the average received SNR from the transmitter located at the cell edge. For LOS and NLOS cases, the reference SNRs are 10 dB and 5 dB, respectively. The number of users to decode, K, is first fixed as two with $T_1 \in \Omega_1, T_2 \in \Omega_2$, and scenarios with more numbers of transmitters follow. Without loss of generality, T_1 is considered as the LOS user while T_2 is regarded as the NLOS user. The simulation parameters are summarized in Table 2. The three V2X schemes are evaluated via PDR, goodput, and data rate performance.

Table 2 – Simulation parameters

Parameter	Value
r	200 m
x_o^{max}	100 m
P_{tx}	10 dBW
$Bandwidth$	10 MHz
α_j	1.67/1.90 for LOS/NLOS
ρ_j	54.85 dB/54.55 dB for LOS/NLOS
N_o	-93 dBm/Hz
Reference SNRs	10 dB/5 dB for LOS/NLOS
β	1 to 10
λ	1 to 215 cars per km

5.1 Impact of interfering vehicular density

In addition to the noise, interference from other transmitters degrades the PDR performance. To study the impact of interference, we vary the density of transmitters in a single subchannel and obtain the analytical and simulation results as shown in Fig. 3. Specifically, we consider the C-V2X resource blocks with 10 MHz bandwidth and 100 ms scheduling period according to the standard [32], and assume 100 subchannels per scheduling period. By fixing the data rate at 1.6 bps/Hz ($\beta = 2$ according to *(8)*), each user can transmit $\frac{10^7 \times 0.1 \times 1.6}{100 \times 8} = 2000$ bytes packet give one subchannel. This is sufficient for not only 344 bytes BSM broadcasting [33] but also the HD 720 video streaming when the transmitter is assigned with 25 subchannels. The interfering vehicular density on each street varies from one car to 215 cars per km (e.g., 0.01 car per km per subchannel to 2.15 cars per km per subchannel). This range is sufficient to study the practical density of interfering vehicles.

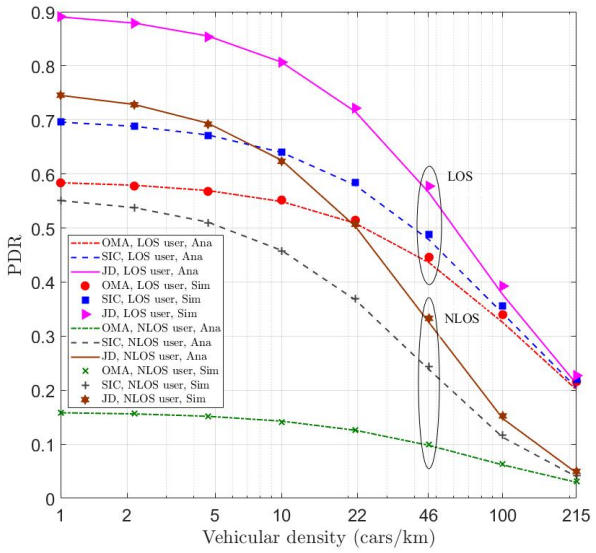

Fig. 3 – PDR under different interfering vehicular density.

For both LOS and NLOS users, the simulation results of the three schemes match with the analytical results. This validates the theoretical analysis in the previous section. The gap in the three schemes decreases as the interfering vehicular density increases. Compared with the NLOS user, the PDR curves of the LOS user are relatively close under the three schemes. In the low interference regime (interfering vehicular density is one car per km), JD provides the highest PDR at 0.9, followed by SIC that shows PDR at 0.7. Compared with the two NOMA schemes, the OMA decoder gives the lowest PDR at around 0.6. When the interfering vehicular density reaches 100 cars per km, the three schemes provide a similar PDR at around 0.34. For the NLOS user, the gap in the three schemes is quite large. The PDR of OMA is lower than 0.2 even in the low interference regime. The two NOMA schemes provide better performance. SIC shows 0.55 PDR in the low interference regime, and JD provides additional 0.2 PDR improvement. Fig. 3 verifies that NOMA can significantly improve the PDR of transmitters suffering from NLOS propagation.

5.2 Impact of data rate

This subsection studies the impact of data rate. For the sake of brevity, the data rate is denoted in unit Mbps give the 10 MHz bandwidth. For instance, the data rate is equivalent to 16 Mbps when $\beta = 2$. We consider interfering vehicular density at 10 cars per km and vary the data rate from 10 to 35 Mbps (i.e., $\beta \in [1, 10]$). Fig. 4 compares the PDR performance of the three schemes.

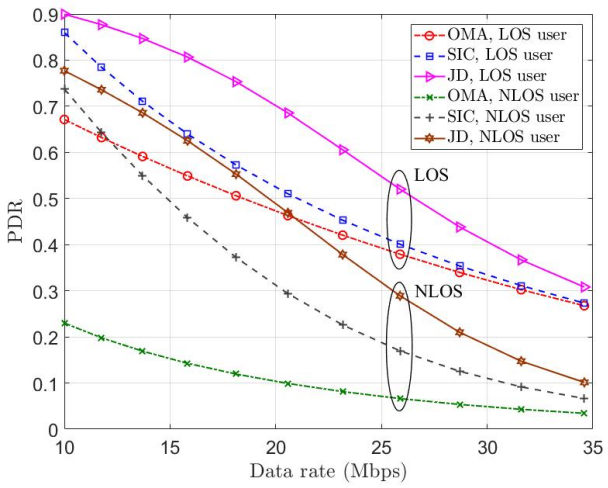

Fig. 4 – PDR under different data rate.

Similar to the study on interfering vehicular density, the OMA scheme shows a low PDR for the NLOS user due to a relatively low received signal strength as compared with the LOS user. The maximum PDR of OMA is lower than 0.23 when the data rate is equal to 10 Mbps. In contrast, the two NOMA schemes have a PDR higher than 0.7 given the same data rate. Since the LOS user can be decoded with a high probability given a low data rate, the PDR of the NLOS user can be improved with either SIC or JD

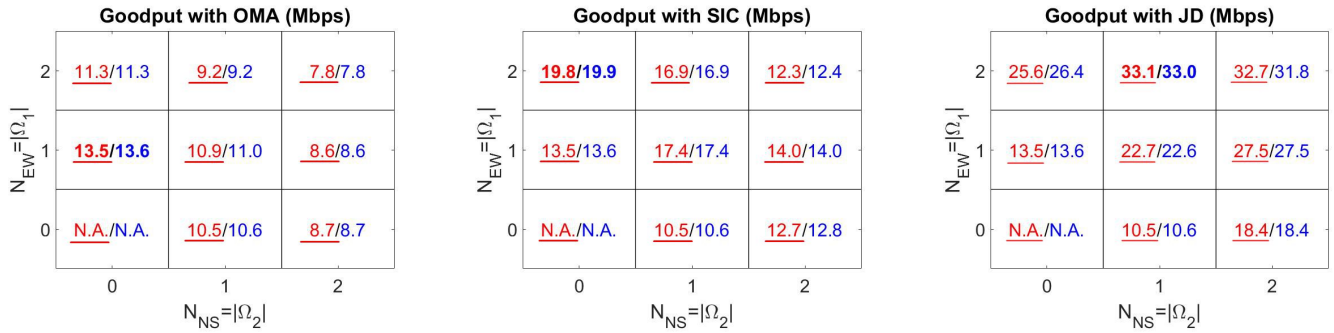

(a) Goodput with OMA. (b) Goodput with SIC. (c) Goodput with JD.

Fig. 5 – Goodput performance under different number of transmitters. The analytical results are denoted by the red text with an underscore and the simulation results are denoted by the blue text without underscore. The maximal goodput results are highlighted with bold text.

receivers. For a high data rate (e.g., 35 Mbps), the three schemes achieve similarly low PDR for the LOS user, thus both the SIC and JD receivers provide not much advantage for the NLOS user. Compared with the SIC scheme, the JD scheme shows around 0.4 and 0.2 PDR enhancements for the LOS and NLOS users, respectively. However, the performance gap between the two NOMA schemes is minor when the data rate is low (e.g., 10 Mbps). The results imply that the JD decoder is preferred for a higher PDR, but the SIC decoder could be a better choice when the data rate is low due to a similar performance and lower complexity.

5.3 Impact of the number of users

After studying the two-user scenario, this subsection evaluates the goodput performance with multiple users. We consider the case with 10 cars per km and $\beta = 2$. The number of transmitters can be set to an arbitrary number according to *(18)* and *(21)*. A road intersection with four segments is the fundamental unit in vehicular networks, thus we focus on the four users' case in this section. The number of transmitters to decode on each street varies from zero to two, and the results up to four users are illustrated in Fig. 5.

The analytical results are denoted by the red text with an underscore while the simulation results are denoted by the blue text without underscore. $N_{NS} = |\Omega_2|$ and $N_{EW} = |\Omega_1|$ denote the number of access users on streets NS (e.g., NLOS users) and EW (e.g., LOS users), respectively. This further conirms that our model is feasible for multiple transmitters. For the three schemes, JD achieves the maximum goodput at 33.1 Mbps in the three-user case, SIC obtains the maximum goodput at 14.7 Mbps with two-user access, and OMA gets the maximum goodput at 13.5 Mbps with single-user access. As a result, JD is the best solution when the number of users is larger than two.

5.4 Optimal data rate and maximum goodput

This subsection is to evaluate the proposed data rate optimization algorithm. We irst consider the two-user case, the optimal data rate and the corresponding maximum goodput are illustrated in Fig. 6 and Fig. 7 respectively.

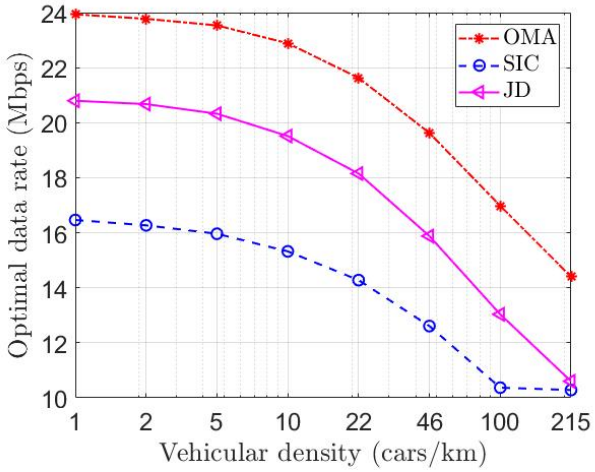

Fig. 6 – Optimal data rate under different interfering vehicular densities.

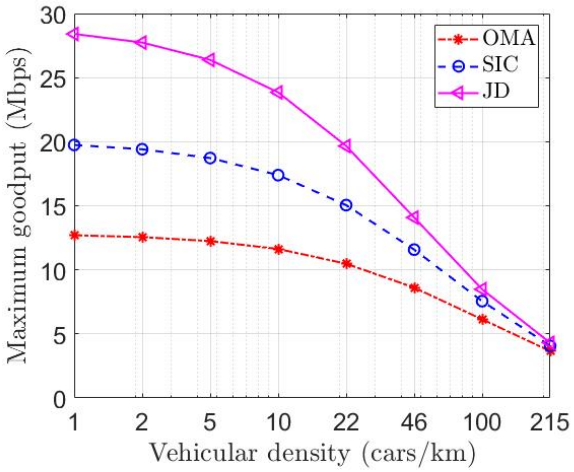

Fig. 7 – Maximum goodput under different interfering vehicular densities.

To maximize the total goodput, we can see that the optimal data rate for the three schemes are $\mathcal{R}_{OMA}^{opt} \geq \mathcal{R}_{JD}^{opt} \geq \mathcal{R}_{SIC}^{opt}$. Applying the optimal data rate, the two NOMA schemes show significant improvement compared with the OMA scheme, especially in the low density regime. When the interfering vehicular density is lower than 10 cars per km, the JD scheme provides more than 100% goodput enhancement compared with the OMA scheme. In the same regime, the SIC scheme shows around 50% improvement. When the interfering vehicular density is equal to 10 cars per km, the goodput distribution of the two-user case under different data rate is shown in Fig. 8. Via exhaustive search, we can observe that the maximum

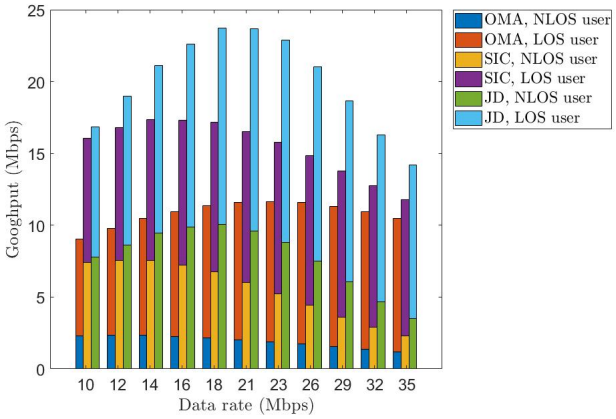

Fig. 8 – Goodput performance under different data rates.

goodput and the corresponding optimal data rate match the results provided by the optimization algorithm. It can be seen that the aggregated goodput first increases as the data rate increases. This means that the interference plus noise is acceptable due to the low data rate, namely low minimum SINR requirement, thus the increasing data rate leads to better goodput performance. After achieving the maximum value, the goodput begins to decreases as the high data rate transmission is sensitive to interference. In this case, a higher data rate leads to lower PDR and worse goodput performance. The distribution of the maximized goodput in Fig. 7 is illustrated in Fig. 9.

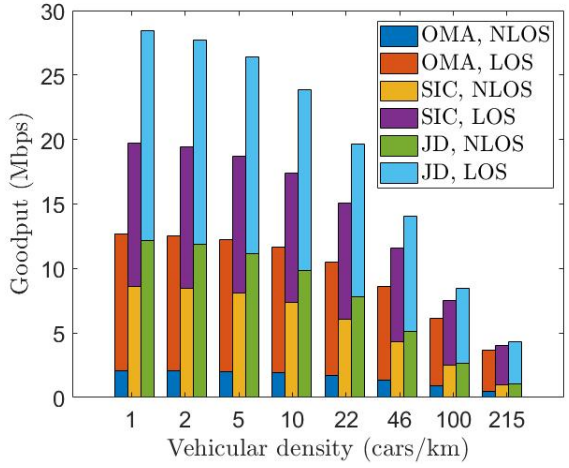

Fig. 9 – Goodput distribution under different interfering vehicular densities.

We have the following observations: 1) the goodput of the NLOS user with OMA receiver is much smaller than others. This is because the OMA scheme applies the highest data rate to maximize the goodput as shown in Fig. 6. In this case, the majority of the goodput comes from the LOS user, and thus the goodput of the NLOS user is relatively low; 2) for both the SIC and JD schemes, it can be observed that the goodput of the LOS and NLOS users is close, especially in the low density regime. It implies that the two NOMA schemes provide better fairness compared with the OMA scheme; 3) in the high density regime, the overall goodput of the three schemes becomes similar, and the goodput mainly comes from the LOS user (the strong user); 4) points 1) to 3) indicate that the development of a hybrid protocol can potentially enhance NOMA-based V2X communications for different communication scenarios.

We then fix the interfering vehicular density at 10 cars per km and study the impact of the number of users. The maximum goodput is shown in Fig. 10. For the OMA scheme, the maximum goodput is achieved with single-user access from street EW. An interesting point is that the maximum goodput of the SIC scheme is the same as that of the OMA scheme, but it can be obtained via not only single-user access but also three-user access (two users from street EW and one user from street NS). It further proves that SIC provides better fairness than OMA. Compared with OMA and SIC, the JD scheme offers much higher goodput, especially for a large number of access users. We can observe that the maximum goodput of JD is achieved in the four-user scenario. For the other two schemes, the maximum goodput is obtained with a smaller number of users. Therefore, it again verifies that the JD scheme is the best choice given a large number of transmitters. For four-user access, the goodput improvement is 375% and 84% when compared with OMA and SIC, respectively. For large-scale vehicular networks, user-grouping with JD enhances the spectrum efficiency by increasing the number of users per group. Due to space limit, the study of user-grouping is left as future work.

5.5 Random access versus collision-free scheduling

So far, the performance is analyzed under the assumption of ALOHA. This subsection considers Collision-Free Scheduled Access (CFSA) that guarantees all users are assigned with the same amount of time-frequency resources with no collision. To avoid collision, CFSA assigns subchannels of the next 100 ms scheduling period when the number of users is larger than 100 (i.e., the number of available subchannels). The CFSA scheme is expected to provide the upper bound of PDR by guaranteeing the orthogonality, and the latency increases linearly with the number of users. The ALOHA-based OMA and CFSA protocols characterize respectively two extreme orthogonal multiple access situations: fully-distributed random access and centralized coordinated control. Fig. 11 to Fig. 14 show the PDR and transmission latency results under LOS and NLOS conditions.

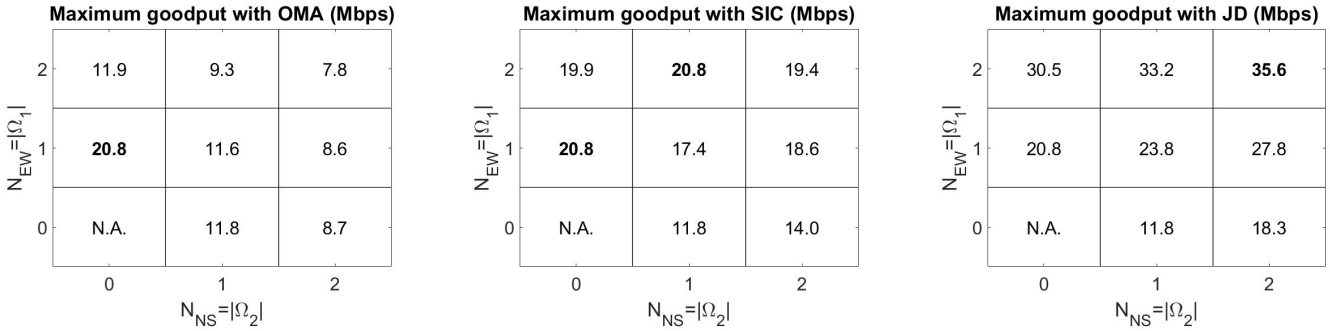

(a) Maximum goodput with OMA. (b) Maximum goodput with SIC. (c) Maximum goodput with JD.

Fig. 10 – Maximum goodput under different numbers of transmitters with the optimal data rate.

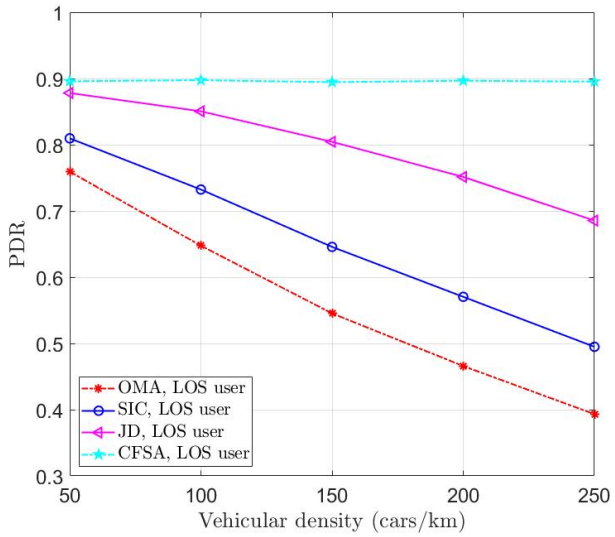

Fig. 11 – PDR against interfering vehicular density under LOS condition.

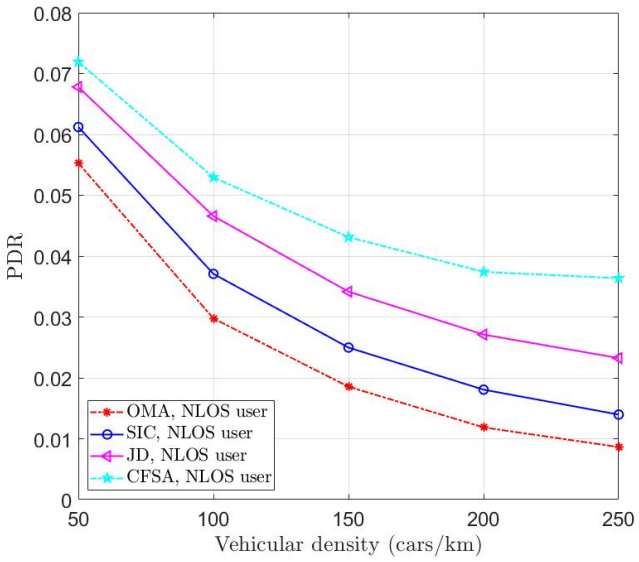

Fig. 12 – PDR against interfering vehicular density under NLOS condition.

We can see from Fig. 11 and Fig. 12 that the PDR of the JD scheme is close to the CFSA scheme when the vehicular density is low, and the gap is only around 0.2 even under the jamming condition (with vehicular density = 250 cars/km) for the LOS case. CFSA shows the lowest transmission latency given low vehicular density for both the LOS and NLOS cases (Fig. 13, 14), since there are sufficient resource channels to be assigned orthogonally. As the vehicular density increases, CFSA allocates the subchannels of the next 100 ms scheduling period, while the two NOMA schemes allow users to share the same subchannel to reduce the latency. For the LOS case in Fig. 13, it turns out that the transmission latency of the JD scheme is lower than CFSA when the vehicular density is beyond 140 cars/km. That is, when the road is over 56% jammed.

6. CONCLUSION

This paper presents a tractable network model to analyze V2X broadcast performance operating in an uncoordinated network. Speci ically, the road intersection scenario is considered and the communications can be divided into two categories: 1) LOS communications between vehicles on the same street; 2) NLOS communications between vehicles on different streets. We have derived the PDR expressions of these two types of communications for various receiving techniques, i.e., the conventional OMA receiver, SIC receiver, and JD receiver. The analytical and simulation results reveal that the NOMA schemes generally outperform the OMA scheme, especially for users suffering from NLOS propagation and long transmission distance. Besides the performance analysis, we have also proposed a data rate optimization scheme to maximize the aggregated goodput. The goodput distribution among the users implies that both the SIC and JD schemes offer good fairness among multiple users, which cannot be achieved by the OMA scheme due to the low PDR of weak users.

Overall, several interesting points are obtained from the results: 1) for applications requiring a high data rate, the JD scheme is always the best choice; 2) for low data rate

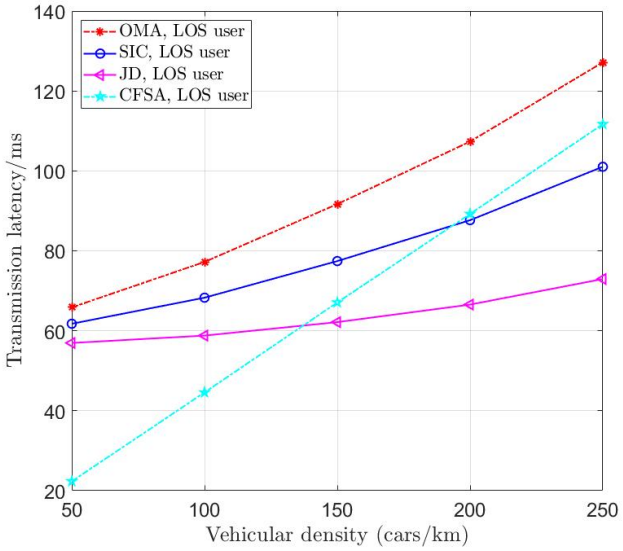

Fig. 13 – Transmission latency against interfering vehicular density under LOS condition.

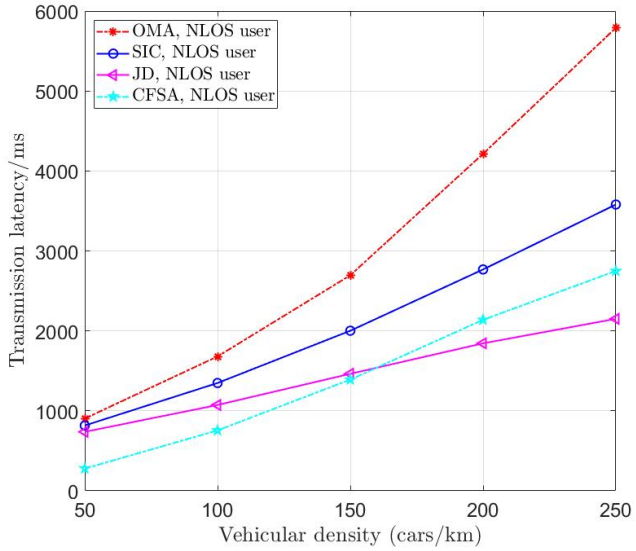

Fig. 14 – Transmission latency against interfering vehicular density under NLOS condition.

applications, the SIC scheme requires relatively low complexity and has similar performance compared with the JD scheme; 3) in the extremely low SINR regime, all the three receiving schemes have similar performance and thus the OMA receiver should be applied due to the lowest complexity; 4) when there are a large number of users (e.g., $K > 2$), JD is the best solution to provide high goodput; 5) as implied from points (1) to (4), we note that the development of a hybrid protocol for NOMA-based V2X communications is critical to meet the requirements of diverse scenarios; and 6) the random access-based NOMA schemes can achieve lower transmission latency than the Collision-Free Scheduled Access (CFSA) scheme in dense vehicular networks. These findings will provide insights into the further development of existing V2X multiple access protocols, and are expected to open up a whole new dimension in real-time vehicular networking for enhancing safety and efficiency in future autonomous cooperative driving.

A. PROOF OF COROLLARY 2

The appendices can be found in [34].

B. PROOF OF COROLLARY 3

The appendices can be found in [34].

REFERENCES

[1] 3rd Generation Partnership Project. “Release 14”. In: *URL http://www.3gpp.org/release-14* (2016).

[2] Boya Di, Lingyang Song, Yonghui Li, and Zhu Han. “V2X Meets NOMA: Non-Orthogonal Multiple Access for 5G-Enabled Vehicular Networks”. In: *IEEE Wireless Communications* 24.6 (2017), pp. 14–21.

[3] SM Riazul Islam, Nurilla Avazov, Octavia A Dobre, and Kyung-Sup Kwak. “Power-domain non-orthogonal multiple access (NOMA) in 5G systems: Potentials and challenges”. In: *IEEE Communications Surveys & Tutorials* 19.2 (2017), pp. 721–742.

[4] Chun Yeen Ho and Chee Yen Leow. “Cooperative Non-Orthogonal Multiple Access with Physical Layer Network Coding”. In: *IEEE Access* (2019).

[5] Mojtaba Vaezi, Gayan Amarasuriya, Yuanwei Liu, Ahmed Arafa, Fang Fang, and Zhiguo Ding. “Interplay Between NOMA and Other Emerging Technologies: A Survey”. In: *arXiv preprint arXiv:1903.10489* (2019).

[6] David Tse and Pramod Viswanath. *Fundamentals of wireless communication*. Cambridge university press, 2005.

[7] Yushu Zhang, Kewu Peng, Jian Song, and Yaqi Sun. “Channel coding for NOMA schemes with a JD or SIC receiver”. In: *2017 13th International Wireless Communications and Mobile Computing Conference (IWCMC)*. IEEE. 2017, pp. 1599–1603.

[8] Lu Lu, Lizhao You, and Soung Chang Liew. “Network-coded multiple access”. In: *IEEE Transactions on Mobile Computing* 13.12 (2014), pp. 2853–2869.

[9] Zhenhui Situ, Ivan Wang-Hei Ho, Taotao Wang, Soung Chang Liew, and Sid Chi-Kin Chau. “OFDM modulated PNC in V2X communications: An ICI-aware approach against CFOs and time-frequency-selective channels”. In: *IEEE Access* 7 (2018), pp. 4880–4897.

[10] Zhenhui Situ and Ivan Wang-Hei Ho. "NO-V2X: Non-orthogonal multiple access with side information for V2X communications". In: *International Conference on Smart Grid Inspired Future Technologies*. Springer. 2018, pp. 133–144.

[11] Zhenhui Situ, Ivan Wang-Hei Ho, Yun Hou, and Peiya Li. "The feasibility of NOMA in C-V2X". In: *IEEE INFOCOM 2020-IEEE Conference on Computer Communications Workshops (INFOCOM WKSHPS)*. IEEE. 2020, pp. 562–567.

[12] Boya Di, Lingyang Song, and Yonghui Li. "Sub-channel assignment, power allocation, and user scheduling for non-orthogonal multiple access networks". In: *IEEE Transactions on Wireless Communications* 15.11 (2016), pp. 7686–7698.

[13] Shengjie Guo and Xiangwei Zhou. "Robust power allocation for NOMA in heterogeneous vehicular communications with imperfect channel estimation". In: *Personal, Indoor, and Mobile Radio Communications (PIMRC), 2017 IEEE 28th Annual International Symposium on*. IEEE. 2017, pp. 1–5.

[14] Jingjing Zhao, Yuanwei Liu, Kok Keong Chai, Yue Chen, and Maged Elkashlan. "Joint subchannel and power allocation for NOMA enhanced D2D communications". In: *IEEE Transactions on Communications* 65.11 (2017), pp. 5081–5094.

[15] L Qian, Yuan Wu, Haibo Zhou, and S Shen. "Dynamic cell association for non-orthogonal multiple-access V2S networks". In: *IEEE J. Sel. Areas Commun* 35.10 (2017), pp. 2342–2356.

[16] Jinho Choi. "NOMA-based random access with multichannel ALOHA". In: *IEEE Journal on Selected Areas in Communications* 35.12 (2017), pp. 2736–2743.

[17] Jun Bae Seo, Bang Chul Jung, and Hu Jin. "Non-Orthogonal Random Access for 5G Mobile Communication Systems". In: *IEEE Transactions on Vehicular Technology* (2018).

[18] Jun-Bae Seo, Bang Chul Jung, and Hu Jin. "Performance Analysis of NOMA Random Access". In: *IEEE Communications Letters* (2018).

[19] Yushu Zhang, Kewu Peng, Zhangmei Chen, and Jian Song. "SIC vs. JD: Uplink NOMA techniques for M2M random access". In: *Communications (ICC), 2017 IEEE International Conference on*. IEEE. 2017, pp. 1–6.

[20] Boya Di, Lingyang Song, Yonghui Li, and Geoffrey Ye Li. "Non-orthogonal multiple access for high-reliable and low-latency V2X communications in 5G systems". In: *IEEE Journal on Selected Areas in Communications* 35.10 (2017), pp. 2383–2397.

[21] Jung-Bin Kim and In-Ho Lee. "Non-orthogonal multiple access in coordinated direct and relay transmission". In: *IEEE Communications Letters* 19.11 (2015), pp. 2037–2040.

[22] Yingyang Chen, Li Wang, Yutong Ai, Bingli Jiao, and Lajos Hanzo. "Performance analysis of NOMA-SM in vehicle-to-vehicle massive MIMO channels". In: *IEEE Journal on Selected Areas in Communications* 35.12 (2017), pp. 2653–2666.

[23] Jeffrey G Andrews, François Baccelli, and Radha Krishna Ganti. "A tractable approach to coverage and rate in cellular networks". In: *IEEE Transactions on communications* 59.11 (2011), pp. 3122–3134.

[24] Zhen Tong, Hongsheng Lu, Martin Haenggi, and Christian Poellabauer. "A Stochastic Geometry Approach to the Modeling of DSRC for Vehicular Safety Communication." In: *IEEE Trans. Intelligent Transportation Systems* 17.5 (2016), pp. 1448–1458.

[25] Muhammad Nadeem Sial, Yansha Deng, Junaid Ahmed, Arumugam Nallanathan, and Mischa Dohler. "Stochastic Geometry Modeling for Uplink Cellular V2X Communication". In: ().

[26] John B Kenney. "Dedicated short-range communications (DSRC) standards in the United States". In: *Proceedings of the IEEE* 99.7 (2011), pp. 1162–1182.

[27] Md Noor-A-Rahim, GG Md Nawaz Ali, Hieu Nguyen, and Yong Liang Guan. "Performance Analysis of IEEE 802.11 p Safety Message Broadcast With and Without Relaying at Road Intersection". In: *IEEE Access* 6 (2018), pp. 23786–23799.

[28] Izrail Solomonovich Gradshteyn and Iosif Moiseevich Ryzhik. *Table of integrals, series, and products*. Academic press, 2014.

[29] George Elmer Forsythe, Cleve B Moler, and Michael A Malcolm. "Computer methods for mathematical computations". In: (1977).

[30] Herman Fernández, Lorenzo Rubio, Vicent M Rodrigo-Peñarrocha, and Juan Reig. "Path loss characterization for vehicular communications at 700 MHz and 5.9 GHz under LOS and NLOS conditions". In: *IEEE Antennas and Wireless Propagation Letters* 13 (2014), pp. 931–934.

[31] Harpreet S Dhillon, Howard Huang, Harish Viswanathan, and Reinaldo A Valenzuela. "Fundamentals of throughput maximization with random arrivals for M2M communications". In: *IEEE Transactions on Communications* 62.11 (2014), pp. 4094–4109.

[32] Rafael Molina-Masegosa and Javier Gozalvez. "LTE-V for sidelink 5G V2X vehicular communications: a new 5G technology for short-range vehicle-to-everything communications". In: *IEEE Vehicular Technology Magazine* 12.4 (2017), pp. 30–39.

[33] Muhammad Awais Javed, Duy Trong Ngo, and Jamil Yusuf Khan. "Distributed spatial reuse distance control for basic safety messages in SDMA-based VANETs". In: *Vehicular Communications* 2.1 (2015), pp. 27–35.

[34] Zhenhui Situ, Ivan Wang-Hei Ho, X. Xu, Y. L. Guan, and L.F. Xie. "Stochastic Analysis of Urban V2X Communications: Orthogonality versus Non-orthogonality: Appendix". In: *URL: http://www.eie.polyu.edu.hk/~whho/Publications/NOV2X_Appendix.pdf* (2019).

AUTHORS

Zhenhui Situ received a Ph.D. degree in electronic and information engineering from The Hong Kong Polytechnic University (PolyU), Hong Kong, in 2020, an M.Sc. degree in electronic engineering from The Hong Kong University of Science and Technology, Hong Kong, in 2014, and a B.S. degree in electronic information science and technology from Sun Yat-sen University, China, in 2013. From 2014 to 2015, he was a research assistant with PolyU. His research interests include wireless communications and statistical signal processing, specifically in vehicular networks. Most of his research focuses on the feasibility study of non-orthogonal multiple access in vehicular networks. He is currently a senior engineer at Huawei Technologies, China.

Ivan Wang-Hei Ho received B.Eng. and M.Phil. degrees in information engineering from The Chinese University of Hong Kong, Hong Kong, in 2004 and 2006, respectively, and a Ph.D. degree in electrical and electronic engineering from Imperial College London, U.K., in 2010. He was a research intern with the IBM Thomas J. Watson Research Center, Hawthorne, NY, USA, and a postdoctoral research associate with the System Engineering Initiative, Imperial College London. In 2010, he cofounded P2 Mobile Technologies Ltd., where he was chief research and development engineer. He is currently an associate professor with the Department of Electronic and Information Engineering, The Hong Kong Polytechnic University, Hong Kong. His research interests include wireless communications and networking, specifically in vehicular networks, intelligent transportation systems, and Internet of Things (IoT). His work on indoor positioning and IoT received the Gold Medal with the Organizer's Choice Award at iCAN in 2020, and the Gold Medal at the International Exhibition of Inventions Geneva in 2021. He is an associate editor for the IEEE Access and IEEE Transactions on Circuit and Systems II.

Xiaoli Xu is with the School of Information Science and Engineering, Southeast University, China. She received her Bachelor of Engineering (First-Class Honours) and Ph.D. degrees from Nanyang Technological University, Singapore, in 2009 and 2015, respectively. From 2015 to 2018, she was a research fellow at the Nanyang Technological University. From 2018 to 2019, she was a postdoctoral research associate at the University of Sydney, Australia. Her research interests include network coding, age of information, vehicular ad-hoc network and UAV communications.

Yong Liang Guan obtained his Ph.D. from Imperial College London, U.K., and Bachelor of Engineering with first class honours from the National University of Singapore. He is a professor of communication engineering at the School of Electrical and Electronic Engineering, Nanyang Technological University (NTU), Singapore, where he leads the Continental-NTU Corporate Research Lab and the successful deployment of the campus-wide NTU-NXP V2X Test Bed. His research interests include coding and signal processing for communication systems and data storage systems. He is an editor for the IEEE Transactions on Vehicular Technology. He is currently an associate vice president of NTU and a distinguished lecturer of the IEEE Vehicular Technology Society.

Cao Ding received a B.Eng. degree in automation from Beijing University of Chemical Technology, Beijing, China, and an M.Sc. degree in electronic and information engineering from The Hong Kong Polytechnic University (PolyU), Hong Kong. He is currently a research assistant with PolyU. His research interests include vehicular networks and Intelligent Transportation Systems (ITS). His research focuses mostly on the digital twin of vehicular networks and intelligent transport systems.